Ciemat 727
Sp ISSN 614-087-X

IRRADIATION OF A VERY FORWARD CALORIMETER IN THE LHC ENVIRONMENT: SOME CONSEQUENCES

Ferrando, A [1]
Josa, M. I. [2]
Malinin, A. [3]
Martínez -Laso [1]
Pojidaev, V. [4]
Salicio, J. M. [1]

[1] CIEMAT, Madrid, Spain (Under CICYT Grant: AEN92-0829)
[2] CERN, Geneva, Switzerland
[3] ITEP, Moscow, Russia
[4] Universita and Sezione INFN di Firenze, Italy

CENTRO DE INVESTIGACIONES
ENERGETICAS, MEDIOAMBIENTALES Y TECNOLOGICAS

MADRID, 1994

CLASIFICACION DOE Y DESCRIPTORES:

440200
664300
RADIATION DETECTORS
CALORIMETRY
CALORIMETERS
HIGH ENERGY PHYSICS
IRRADIATION
HADRONS

Toda correspondencia en relación con este trabajo debe dirigirse al Servicio de Información y Documentación, Centro de Investigaciones Energéticas, Medioambientales y Tecnológicas, Ciudad Universitaria, 28040-MADRID, ESPAÑA.

Las solicitudes de ejemplares deben dirigirse a este mismo Servicio.

Los descriptores se han seleccionado del Thesauro del DOE para describir las materias que contiene este informe con vistas a su recuperación. La catalogación se ha hecho utilizando el documento DOE/TIC-4602 (Rev. 1) Descriptive Cataloguing On-Line, y la clasificación de acuerdo con el documento DOE/TIC.4584-R7 Subject Categories and Scope publicados por el Office of Scientific and Technical Information del Departamento de Energía de los Estados Unidos.

Este trabajo se ha recibido para su impresión en Octubre de 1993

Depósito Legal nº M-33000-1993
ISBN 84-7834-200-1
ISSN 614-087-X
NIPO 238-94-024-1

IMPRIME CIEMAT

1. INTRODUCTION.

The Very Forward Calorimeter of CMS [1] (LHC Compact Solenoidal Detector) extends the hermetic coverage up to $|\eta| = 5$, allowing very forward jet tagging [2] and improvement of the E_T^{miss} resolution [3]. These features are essentially related to "high mass" Higgs production and Supersymmetry search. However, at the LHC, more than 80% of the total pp production cross-section will flow in the very forward direction ($|\eta| > 2.5$). The device will then be irradiated by a high flux of particles.

In this work, we have investigated the levels of expected irradiation and induced radioactivity in the Very Forward Calorimeter using Monte-Carlo techniques.

In this report, we give in Section 2 a short description of the device. In Section 3 we present the Monte-Carlo samples. Section 4 shows the expectations in terms of irradiation. Levels of induced activity in the absorber are discussed in Section 5. The consequences of tritium production are given in Section 6, and some conclusions are drawn in Section 7.

2. DESIGN AND MECHANICS.

The Very Forward Calorimeters (VFWC's) will be located 11 m away from the interaction region (IR) of the CMS detector (fig.1). They will cover the pseudorapidity region $2.5 < |\eta| < 4.7$. A transverse view of CMS is shown in fig. 2.

Each VFWC consists of six walls of dimensions X*Y*Z = 4.4x4.4x0.40 m^3, leaving a central hole X*Y*Z = 0.40x0.40x0.40 m^3, for the beam pipe. Fig. 3 gives an artist view of one VFWC.

Each wall is assembled from modules of Parallel Plate Volumes, or "bricks", of dimensions X*Y*Z = 20x40x40 cm^3. Each of these Volumes consists of a stainless steel box containing a series of 21 iron planes, of dimensions 20x40x1.7 cm^3, interleaved with 1.5 mm gaps provided by ceramic spacers. Fig. 4 shows a full size prototype Volume under construction. It has an equivalent length of 2 λ_I (around 20 X_0). The weight of such a unit is about 225 kg.

Details concerning operation and expected performance of such a calorimeter can be found elsewhere [4-6].

3. MONTE-CARLO STUDIES.

3.1. Generation of events.

For simulation purposes we have assumed the scenario given in fig. 2, where a schematic view of a quarter of CMS is shown. The total VFWC volume is 4.4x4.4x2.5 m^3 with a 0.4x0.4x2.5 m^3 central hole.

We have simulated minimum bias pp collisions at a center of mass energy of 16 TeV.

The generator used in this simulation was ISAJET [7]. We call "Minimum Bias Crossing" a mixture of 80% Minimum Bias (MB) and 20% Two Jet (TJ) pp collisions, found in the past to be the best representation of the Minimum Bias data at the SppS Collider.

The luminosity was taken equal to 1.7×10^{34} cm^{-2} s^{-1} and the bunch spacing to 15 ns. The corresponding mean number of pp collisions per crossing is approximately 14.5, following a Poisson distribution (fig. 5 a).

The generated multiplicity distribution per collision is given in fig. 5 b). The peak around 100 corresponds to the MB events and the one around 200 to the TJ events. The small peak on the left corresponds to elastic scattering events, also present in the mixture.

The multiplicity distribution per crossing is given in fig. 5 c). About 3000 stable particles emerge from the IR. The collision point was generated independently for each pp interaction in a crossing. Gaussian distributions with σ_x = 0.001 cm, σ_y = 0.001 cm and σ_z = 5.0 cm, around $x_o = y_o = z_o = 0$, were used. Fig. 6 illustrates this point.

We have generated 4000 MB and 1000 TJ events for a total of 1000 crossings.

The nominal magnetic field map for the solenoide was used to swim the charged particles emerging from the IR. Vacuum was the material considered in front of the VFWC.

We have assumed that a particle reaching the central and forward regions in fig. 2 will not hit the entry face of the VFWC. This central/forward region is defined as a cylinder, having 1.3 m in radius and extending from -10 m to 10 m in Z around IR, Z being the beam line.

3.2. Simulation of the Very Forward Calorimeter.

We have considered that particles produced at the IR and reaching the VFWC will develop showers in the iron. Only hadronic showers are relevant for the present study.

For cascade simulation the VFWC is seen as a volume consisting of 120 iron plates of dimensions 4400x4400x17 mm^3 each, interleaved with gas gaps of 1.5 mm. Every plate is subdivided into 1936 cells, 100x100 mm^2 each, simulating the electrodes.

We have used GEANT 3.15 [8] to generate showers in the VFWC and to calculate the production rates of protons, neutrons, charged pions and tritium in the iron. FLUKA [9] was used as the hadron shower generator. Secondary particles were tracked down to 10 keV in steps of 0.1 mm in the iron.

4. IRRADIATION.

The dN/dE distribution of the outgoing particles is given in fig. 7 a). The average energy per particle is 78 GeV. About 70% of the secondary particles reach the VFWC's front face, with a mean energy of 111 GeV per particle (see fig. 7b). About 50% of them hit the VFWC's sensitive areas (fig. 7c), with an average energy of about 6 GeV per particle. The remaining 50% of the particles pass through the central VFWC's holes. Notice that all the particles with $E > 1$ TeV go through the holes. The same is also true for charged particles having less than 0.5 GeV, due to magnetic field effects [10].

The energy flow is very correlated with $|\eta|$ [10]. For irradiation studies we have divided the VFWC into three regions: $2.5 < |\eta| < 3$, $3 < |\eta| < 4$ and $4 < |\eta| < 4.7$. These intervals correspond to the geometrical regions shown in fig. 3. The inner area expands up to 20 cm away from the central hole. The intermediate region goes from 20 cm to 80 cm and the outer one from 80 cm to 220 cm. The corresponding expected distributions of the total collected energy, per crossing, at the various $|\eta|$ regions (one VFWC side only), are given in fig. 8 a) to c).

For $|\eta| < 3$, the averaged collected energy per crossing is of the order of 200 GeV. It reaches 1.2 TeV in the region $3 < |\eta| < 4$ and 1.6 TeV in the inner region.

About 525 stable particles hit the sensitive area of the VFWC (one side) per crossing. From them, 293 are charged pions, 13 are protons and antiprotons (p), and around 8.4 are neutrons and antineutrons (n). The remaining particles are mainly γ's coming from π^o or η decays.

The energy distributions per particle and η regions, are given in figs. 9 to 11 for $\pi^{\pm}$, p and n. We summarize in table 1 the mean values of multiplicities and average energies, for the various particles in the three $|\eta|$ regions. The density of particles and the mean energy increase with $|\eta|$.

The corresponding rates (in Hertz), for the three most copiously produced hadrons in the various regions of the VFWC (one side only), are listed in table 2.

5.ACTIVATION.

The information on the average energy carried by hadrons at the different $|\eta|$ regions has been used to develop showers in the calorimeter. As explained in 3.2., GEANT 3.15 has been used for this study. We have generated 500 showers of each type listed in table 1.

For this calculation, we have considered, in addition to the 3 $|\eta|$ regions, 3 sections in depth, each of them having 4 λ_I in length (2 consecutive walls in fig. 3). Section 1 (S1) will be the nearest to the IR and Section 3 (S3) the farest one.

For this purpose, the VFWC is seen as the composition of 9 volumes. The three outer ones ($|\eta| < 3$: S1, S2, S3), have $12.3*10^6$ cm^3 of iron each. The intermediate volumes have $2.7*10^6$ cm^3 and the three inner ones $3.8*10^5$ cm^3.

To compute the induced radioactivity due to the incoming flux of hadrons, we have studied the production of $\pi^{\pm}$, p and n in the iron (in cm^{-3} s^{-1}) and, following Ref. [11], have extracted the density rate of "stars" produced in the absorber. Stars are defined as charged pions, neutrons with $E_{kinetic} > 50$ MeV and protons with $E_{kinetic} > 20$ MeV.

The conversion factor, from the density rate of produced stars (cm^{-3} s^{-1}) to induced radioactivity in iron [11] is taken as:

$$\omega(30,1) = 10^{-8} \text{ Sv/h per } cm^{-3}\ s^{-1},$$

in units of dose rate after a uniform irradiation during 30 days followed by 1 day of cooling down.

Hadron interactions in the gas were neglected in the calculations since: 1) the gas circulates, 2) the gas/iron ratio is less than 1/10 in volume and about 1/10000 in density.

As an example, we present in fig. 12, the $dn/dE_{kinetic}$ distributions of $\pi^{\pm}$, p, n and ^3H (also included in the GEANT showers) generated in a cascade produced by a 8.1 GeV incoming π^-. Mean values of the distributions are 497.2 MeV, 35.7 MeV, 6.9 MeV and 6.9 MeV for $\pi^{\pm}$, p, n and ^3H respectively. The corresponding multiplicity distributions are given in fig. 13 a) to d), with mean values: 9.9, 13.0, 12.6 and 1.2, respectively.

The average multiplicities were combined with the expected incoming fluxes given in table 2, to derive $\pi^{\pm}$, p and n density production rates in the iron and the corresponding induced activities.

We give in table 3 the expected mean density rates for neutrons, protons and charged pions, in the iron, for the three $|\eta|$ regions and the three sections in depth.

Neutrons will be the most copiously produced particles. Due to the low mean energy of the particles hitting the VFWC most of the showers are made of elastic scattering with nucleons.

The density rates for star production and the induced radioactivity in the iron are listed in table 4. The activity is computed for a 30 days machine operation followed by 1 day cooling down.

As expected, the most activated region is the first section of the inner part ($4 < |\eta| < 4.7$), where, the activity reaches about 6 mSv/h. For the sake of comparison, let us recall that the annual limit [11] for people working at CERN and being controlled by individual monitoring is 15 mSv. In general, the ambient dose rate in the VFWC neighbourhood will largely exceed the 2.5 μSv/h of the so called Control Radiation Areas.

The primary irradiation is not uniform, but increases with $|\eta|$. Thus, the outer faces of the calorimeter (apart from the front one) present less irradiation/activation, allowing installation of electronics and, perhaps, access to it.

Our calculations are in fair agreement with those quoted in Ref. [11].

6. TRITIUM PRODUCTION.

In addition to the production of stars, we have calculated the expected density production rate of ^3H nucleids in the iron. Tritium is one of the longest lived produced radionucleid, with $T_{1/2}$ = 12.4 years. The purpose is to make an estimation of the activity after a given operation time of LHC and infer whether or not the VFWC's have to be considered as radioactive wastes after several years of use in the LHC environment.

Assuming that over 1 year, the machine operates only during 1/3 of the time, the number of tritium nucleids present in the iron, per cm^3, after t years of LHC operation will be:

$$N(t) = (v/\lambda)\ (e^{-2\lambda/3} - e^{-\lambda})\ \Sigma\ e^{-\lambda(i-1)}$$

where $\lambda = \ln 2/T_{1/2}$ and v is the star density production rate (given in $cm^{-3}\ y^{-1}$).

We give in table 5 the ^3H activity after a 10 years operation. The numbers for the activity in table 5, have to be multiplied by 0.95, 0.85 and 0.57, after 1, 3 and 10 years disposal respectively. It will take about 12 years disposal to get activity levels lower by a factor 2 and 40 years to decrease by a factor 10.

Our results are about one order of magnitude lower than those quoted in Ref. [11] for lead. This corresponds to the difference in tritium production cross-section in both materials. It nevertheless shows that, concerning tritium activity, some parts of the VFWC's will have to be considered as active waste once the detector is dismantled. They will exceed the 10^2 Bq/g limit.

In addition to tritium, any star will probably create a radioactive nucleus. Thus, the final saturation activity will be given by the star density production rate and the tritium production. It is then clear that, for the assumed luminosity, at least the inner parts of the VFWC's will be hazardous material to be kept at the CERN site after operation has come to an end.

7. SUMMARY AND CONCLUSIONS.

We have investigated the expected irradiation/activation levels in various regions of a proposed Very Forward Calorimeter in the LHC environment (CMS scheme). Previous research in this domain were already reported by the CERN's TIS-RP Division [11]. Here we have used a different approach, generating primary particles via ISAJET and cascades from GEANT simulation in the calorimeter.

We arrive to the following general conclusions concerning induced activity in the VFWC of the CMS setup:

The activities in the inner regions of the calorimeters will exceed tolerable limits for human beings after a period of operation of 30 days, when the luminosity is assumed to be about $1.7 \times 10^{34}\ cm^{-2}\ s^{-1}$. Under these conditions, the use of robots in the area has to be considered to replace some human interventions.

In addition, we observe that, after operation (10 years), the VFWC's will contain some parts which are likely to be considered as radioactive wastes.

However, the proposed calorimeter has some basic good properties:

i) The active medium, being a circulating gas, is less affected by radiation effects.

ii) The proposed solid materials (iron and ceramics) are most resistent to the activation. In particular, the specific activity (Bq/g) after operation, due to tritium production, will be a factor 10 lower using iron than using lead, for the passive media in the calorimeter.

iii) The modular construction gives the possibility of "shape changing" according to the luminosity. In addition, any "brick" in the structure may be accessed by an externally operated robot system, making replacements possible.

iv) The electronics can be located in non irradiated/activated regions, where human intervention is still possible.

ACKNOWLEDGEMENTS.

We are indebted to M. Aguilar-Benitez, A. Givernaud, K. Lassila-Perini, H. Plothow-Besch and V. Vuillemin, for help and fruitful discussions.

REFERENCES.

[1] "CMS: The Compact Muon Solenoid", Letter of Intent.
The CMS Collaboration, CERN/LHCC 92-3, October 1992.

[2] "Jets at the Very Forward Region of CMS".
A. Ferrando et al., CMS TN/92-22, July 1992.

[3] "The role of the Very Forward Calorimetry in the measurement of the Total and Missing Transverse Energy at CMS".
A. Ferrando et al., CMS TN/92-40, October 1992.

[4] "Notes for a CMS Letter of Intent concerning: very forward jet tagging simulation, very forward calorimetry and forward muon trigger".
A. Ferrando et al., CMS TN/92-23, July 1992.

[5] "Construction and Performance of Parallel Plate Chambers Prototypes".
A. Arefiev et al., RD5 TN/92-04, August 1992.

[6] "Performances of a Parallel Plate Chamber Cell Prototype based on the thick iron technology".
A. Bizzeti et al., RD5 TN/92-05, October 1992.

[7] ISAJET Monte-Carlo.
F. Paige and S. Protopopescu, BNL 38774 (1986).

[8] GEANT3 User's Guide.
R. Brun et al., CERN-DD/EE/84-1 (1987).

[9] "Hadronic Cascade Simulation in GEANT".
K. Lassila, CERN-CN/91/13, December 1991.

[10] "The Minimum Bias environment in the Very Forward region of CMS".
A. Ferrando et al., CMS TN/92-21, July 1992.

[11] "The Estimation of Parameters of Radiological Interest in and around an LHC Experimental Area".
G.R. Stevenson et al, CERN/TIS-RP/IR/92-06, February 1992.

	$2.5 < \|\eta\| < 3$		$3 < \|\eta\| < 4$		$4 < \|\eta\| < 4.7$	
particle	<mult.>	<E>	<mult.>	<E>	<mult.>	<E>
$\pi^{\pm}$	45	2.0	151	3.9	97	8.1
p	1.9	3.5	6.6	6.5	4.5	13.6
n	1.1	5.9	4.5	8.8	2.8	20.3

Table 1

Mean multiplicities and average energy per particle (in GeV), in a crossing, at the three $|\eta|$ regions of the VFWC (one side only) mentioned in the text.

	Rates (s^{-1})			
particle	all	$2.5 < \|\eta\| < 3$	$3 < \|\eta\| < 4$	$4 < \|\eta\| < 4.7$
$\pi^{\pm}$	1.96×10^{10}	3.02×10^{9}	1.01×10^{10}	6.47×10^{9}
p + pbar	8.71×10^{8}	1.27×10^{8}	4.62×10^{8}	3.02×10^{8}
n + nbar	5.63×10^{8}	7.37×10^{7}	3.02×10^{8}	1.88×10^{8}

Table 2

Frequency of hadrons reaching the VFWC sensitive area (one side only).

$\|\eta\|$ region	Section in depth	Volume cm^3	$<n>$ $cm^{-3}\ s^{-1}$	$<p>$ $cm^{-3}\ s^{-1}$	$<\pi^{\pm}>$ $cm^{-3}\ s^{-1}$
$2.5<\|\eta\|<3$	1	$12.3x10^6$	$3.54x10^4$	$3.01x10^3$	$9.17x10^2$
	2	$12.3x10^6$	$1.06x10^4$	$4.36x10^2$	$4.26x10^1$
	3	$12.3x10^6$	$2.03x10^3$	$4.06x10^1$	$0.79x10^0$
$3<\|\eta\|<4$	1	$2.7x10^6$	$9.27x10^5$	$8.08x10^4$	$2.13x10^4$
	2	$2.7x10^6$	$3.17x10^5$	$1.31x10^4$	$1.10x10^3$
	3	$2.7x10^6$	$5.66x10^4$	$1.28x10^3$	$1.41x10^1$
$4<\|\eta\|<4.7$	1	$3.8x10^5$	$6.70x10^6$	$5.84x10^5$	$1.78x10^5$
	2	$3.8x10^5$	$2.81x10^6$	$1.35x10^5$	$1.63x10^4$
	3	$3.8x10^5$	$5.50x10^5$	$1.27x10^4$	$8.11x10^2$

Table 3

Total mean density production rate of hadrons in the iron.

$\|\eta\|$ region	Section in depth	< stars > $cm^{-3}\ s^{-1}$	< Activity > $\mu Sv/h$
$2.5 < \|\eta\| < 3$	1	2.83×10^{3}	2.83×10^{1}
	2	3.16×10^{2}	3.16×10^{0}
	3	2.16×10^{1}	2.16×10^{-1}
$3 < \|\eta\| < 4$	1	7.26×10^{4}	7.26×10^{2}
	2	8.41×10^{3}	8.41×10^{1}
	3	7.38×10^{2}	7.38×10^{0}
$4 < \|\eta\| < 4.7$	1	5.60×10^{5}	5.60×10^{3}
	2	9.41×10^{4}	9.41×10^{2}
	3	7.87×10^{3}	7.87×10^{1}

Table 4

Mean density production of stars in the iron and the corresponding induced radioactivity (one VFWC), after 30 days of machine operation and 1 day cooling.

$\|\eta\|$ region	Section in depth	Mass g	$<^3H>$ $cm^{-3}s^{-1}$	Total Activity Bq	Specific Activity Bq/g
$2.5< \|\eta\| <3$	1	$9.68x10^7$	$3.96x10^1$	$6.58x10^7$	$6.8x10^{-1}$
	2	$9.68x10^7$	$5.16x10^0$	$1.89x10^6$	$8.9x10^{-2}$
	3	$9.68x10^7$	$3.4x10^{-1}$	$1.77x10^4$	$5.9x10^{-3}$
$3< \|\eta\| <4$	1	$2.12x10^7$	$2.02x10^3$	$3.39x10^9$	$3.5x10^1$
	2	$2.12x10^7$	$1.60x10^2$	$5.94x10^7$	$2.8x10^0$
	3	$2.12x10^7$	$4.36x10^1$	$2.25x10^6$	$7.5x10^{-1}$
$4< \|\eta\| <4.7$	1	$3.00x10^6$	$1.16x10^4$	$1.9x10^{10}$	$2.0x10^2$
	2	$3.00x10^6$	$6.61x10^3$	$2.33x10^9$	$1.1x10^2$
	3	$3.00x10^6$	$2.77x10^2$	$1.44x10^7$	$4.8x10^0$
Total	---	$3.63x10^8$	---	$2.5x10^{10}$	---

Table 5

Tritium density production rate in the iron and corresponding activities after a 10 years of LHC operation (see text).

FIGURE CAPTIONS.

Fig. 1: Artist view of the CMS detector with the VFWC location.

Fig 2: Transverse view of one quarter of CMS.

Fig. 3: Sketch of a VFWC. Marks correspond to the three $|\eta|$ regions discussed in the text.

Fig. 4: Drawing of a 21 iron planes Parallel Plate Volume prototype under construction.

Fig. 5:
a) Distribution of the number of collisions per crossing.
b) Multiplicity distribution per collision.
c) Multiplicity distribution per crossing.

Fig. 6: Distribution of the collision coordinates:
a) Xo.
b) Yo.
c) Zo.

Fig. 7: dN/dE distributions for stable particles:
a) At the interaction region (all data).
b) At the VFWC front plane (two sides).
c) At the VFWC sensitive area (one side).

Fig. 8: Expected total energy distribution per crossing at the VFWC entry face (one side only), for:
a) $|\eta| < 3$.
b) $3 < |\eta| < 4$.
c) $4 < |\eta| < 4.7$.

Fig. 9: dn/dE distributions for the $\pi^{\pm}$'s reaching the VFWC sensitive area (one side only):
a) full distribution.
b) for $|\eta| < 3$.
c) for $3 < |\eta| < 4$.
d) for $4 < |\eta| < 4.7$.

Fig. 10: Same as in Fig. 10, for p's.

Fig. 11: Same as in Fig. 10, for n's.

Fig.12: $dn/dE_{kinetic}$ distributions for secondary particles in a 8.1 GeV π^- shower:

a) $\pi^{\pm}$'s.
b) p's.
c) n's.
d) ^3H nucleids.

Fig.13: Multiplicity distributions in a 8.1 GeV π^- shower, for:

a) $\pi^{\pm}$'s.
b) p's.
c) n's.
d) ^3H nucleids.

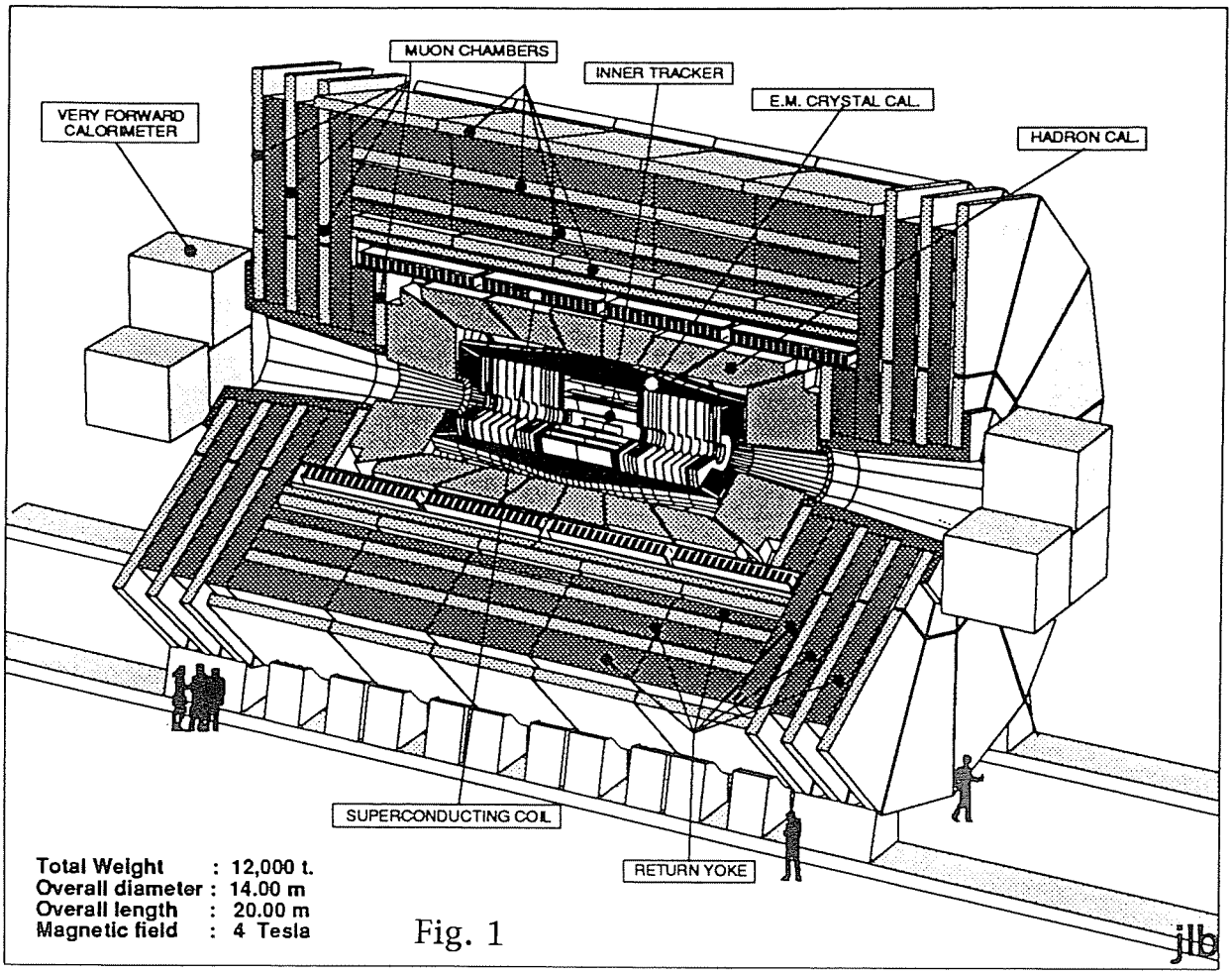
MUON CHAMBERS
INNER TRACKER
E.M. CRYSTAL CAL.
HADRON CAL.
VERY FORWARD CALORIMETER
SUPERCONDUCTING COIL
RETURN YOKE
Total Weight : 12,000 t.
Overall diameter : 14.00 m
Overall length : 20.00 m
Magnetic field : 4 Tesla
jlb

Fig. 1

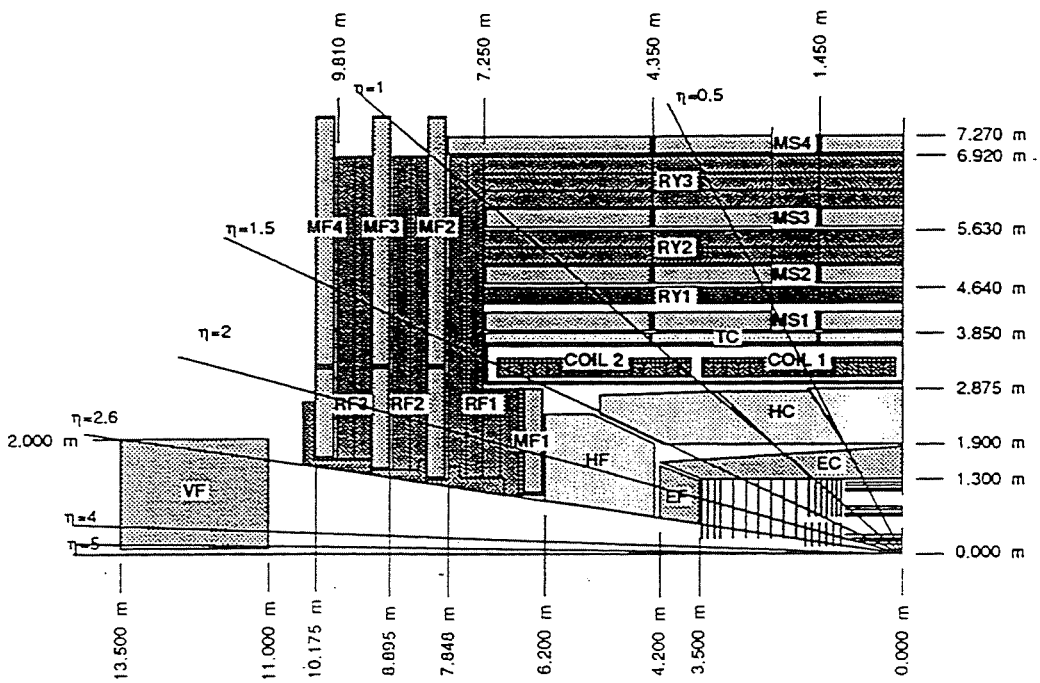
9.810 m
7.250 m
4.350 m
1.450 m
η=1
η=0.5
η=1.5
η=2
η=2.6
η=4
η=5
2.000 m
MF4
MF3
MF2
RF3
RF2
RF1
MF1
VF
HF
EF
MS4
RY3
MS3
RY2
MS2
RY1
MS1
TC
COIL 2
COIL 1
HC
EC
7.270 m
6.920 m
5.630 m
4.640 m
3.850 m
2.875 m
1.900 m
1.300 m
0.000 m
13.500 m
11.000 m
10.175 m
8.095 m
7.848 m
6.200 m
4.200 m
3.500 m
0.000 m

Fig. 2

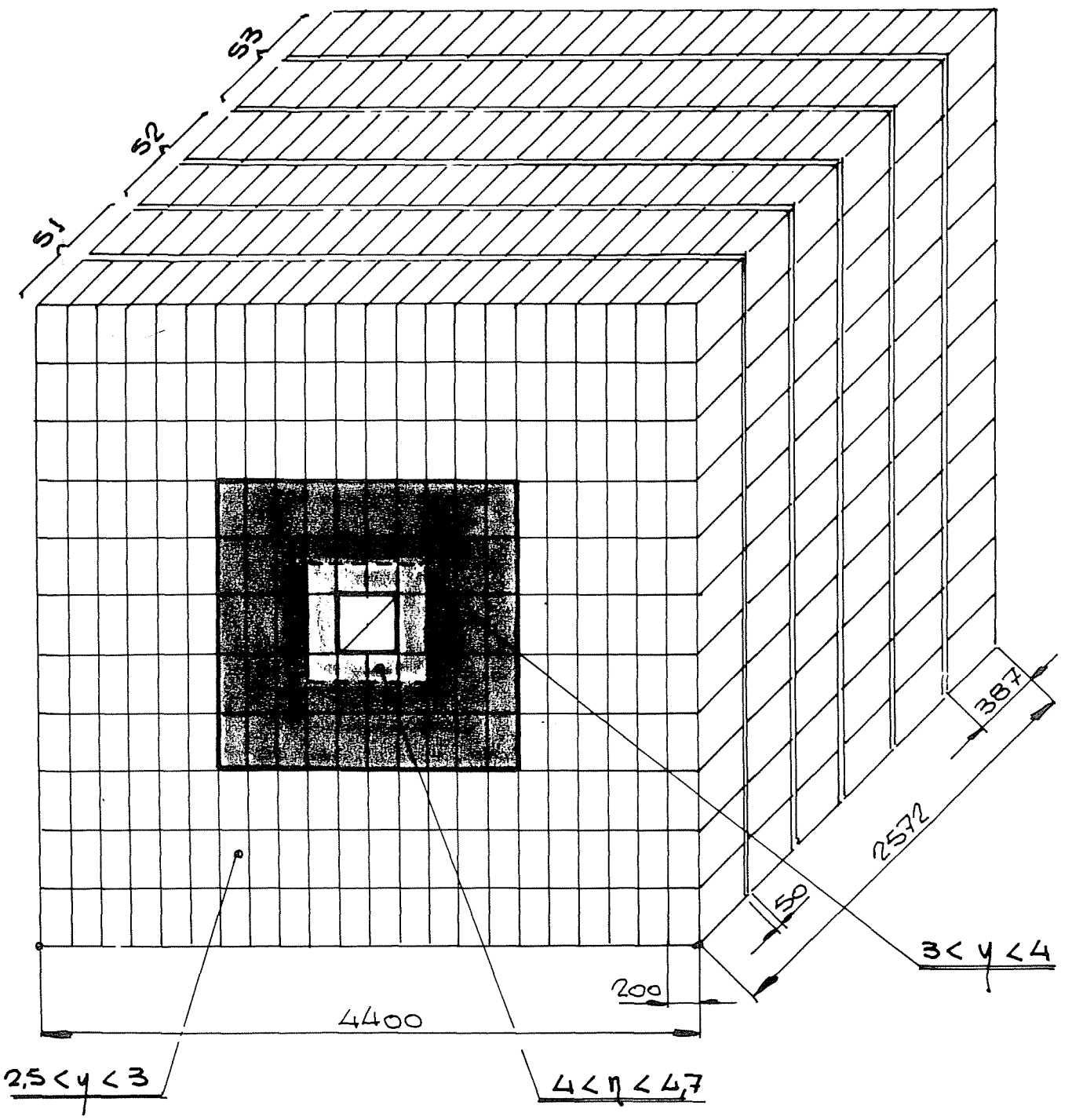

Fig. 3

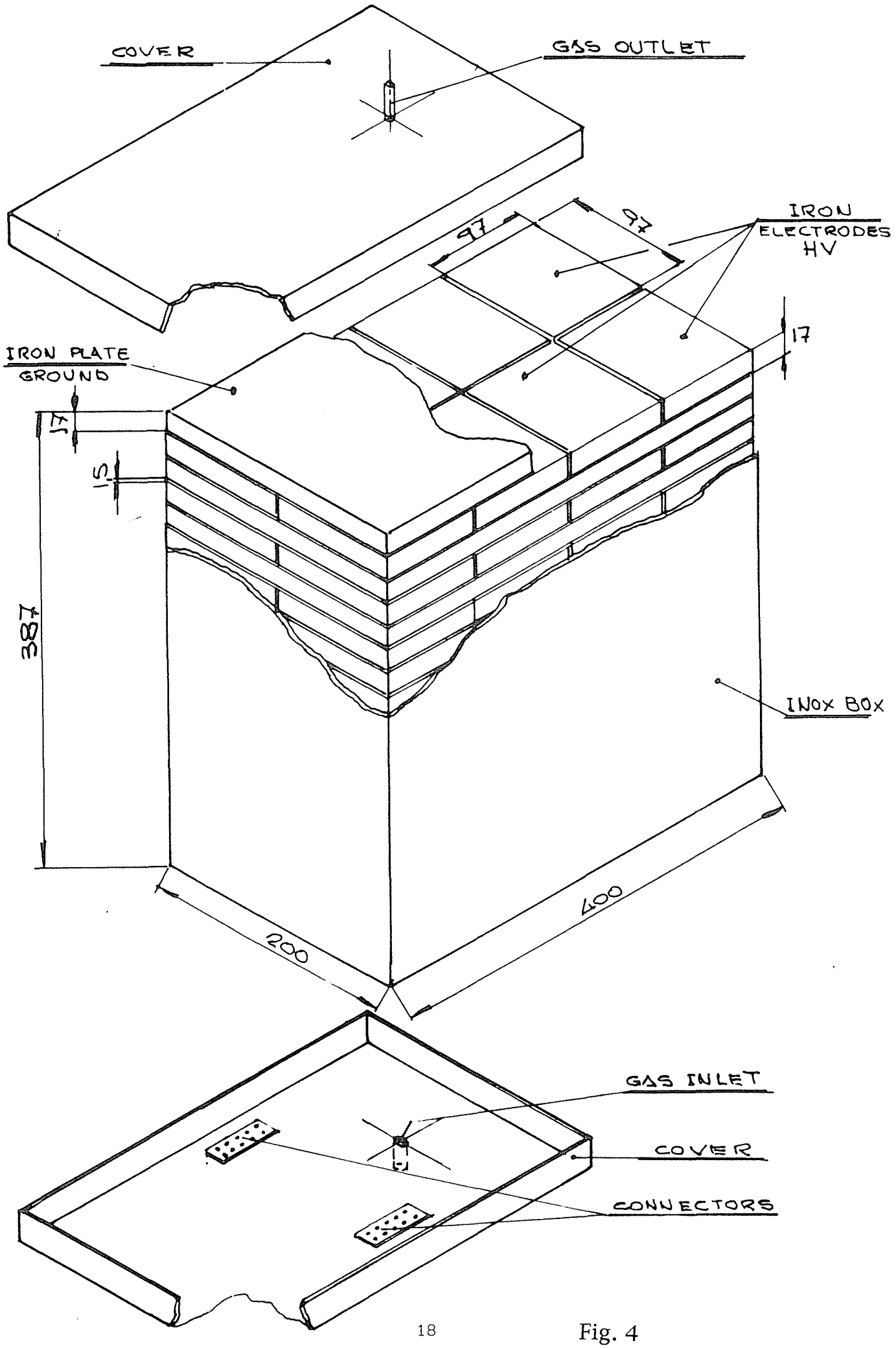
COVER
GAS OUTLET
IRON
ELECTRODES
HV
97
97
17
IRON PLATE
GROUND
17
5
387
INOX BOX
200
400
GAS INLET
COVER
CONNECTORS

Fig. 4

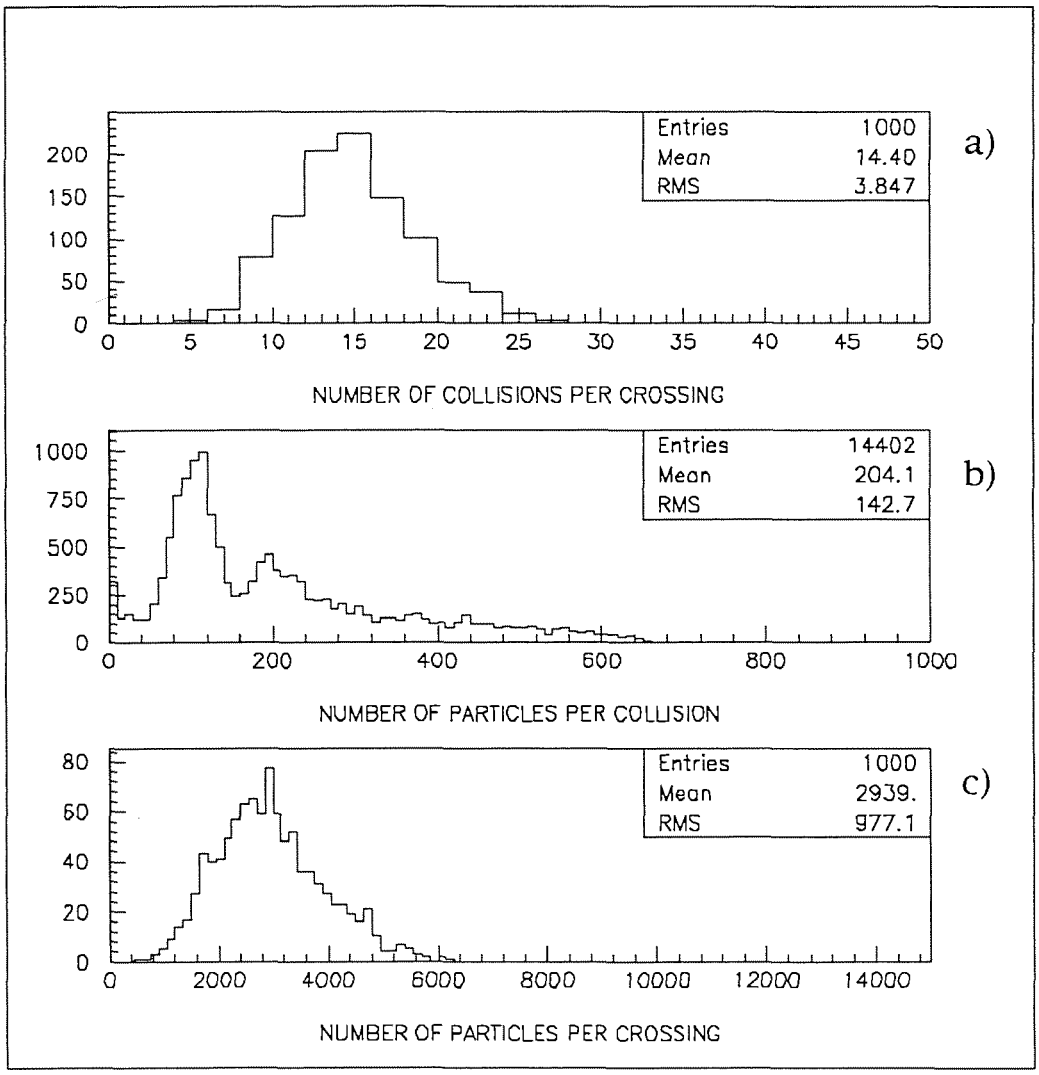
Entries 1000
Mean 14.40
RMS 3.847
a)
200
150
100
50
0
0 5 10 15 20 25 30 35 40 45 50
NUMBER OF COLLISIONS PER CROSSING
Entries 14402
Mean 204.1
RMS 142.7
b)
1000
750
500
250
0
0 200 400 600 800 1000
NUMBER OF PARTICLES PER COLLISION
Entries 1000
Mean 2939.
RMS 977.1
c)
80
60
40
20
0
0 2000 4000 6000 8000 10000 12000 14000
NUMBER OF PARTICLES PER CROSSING

Fig. 5

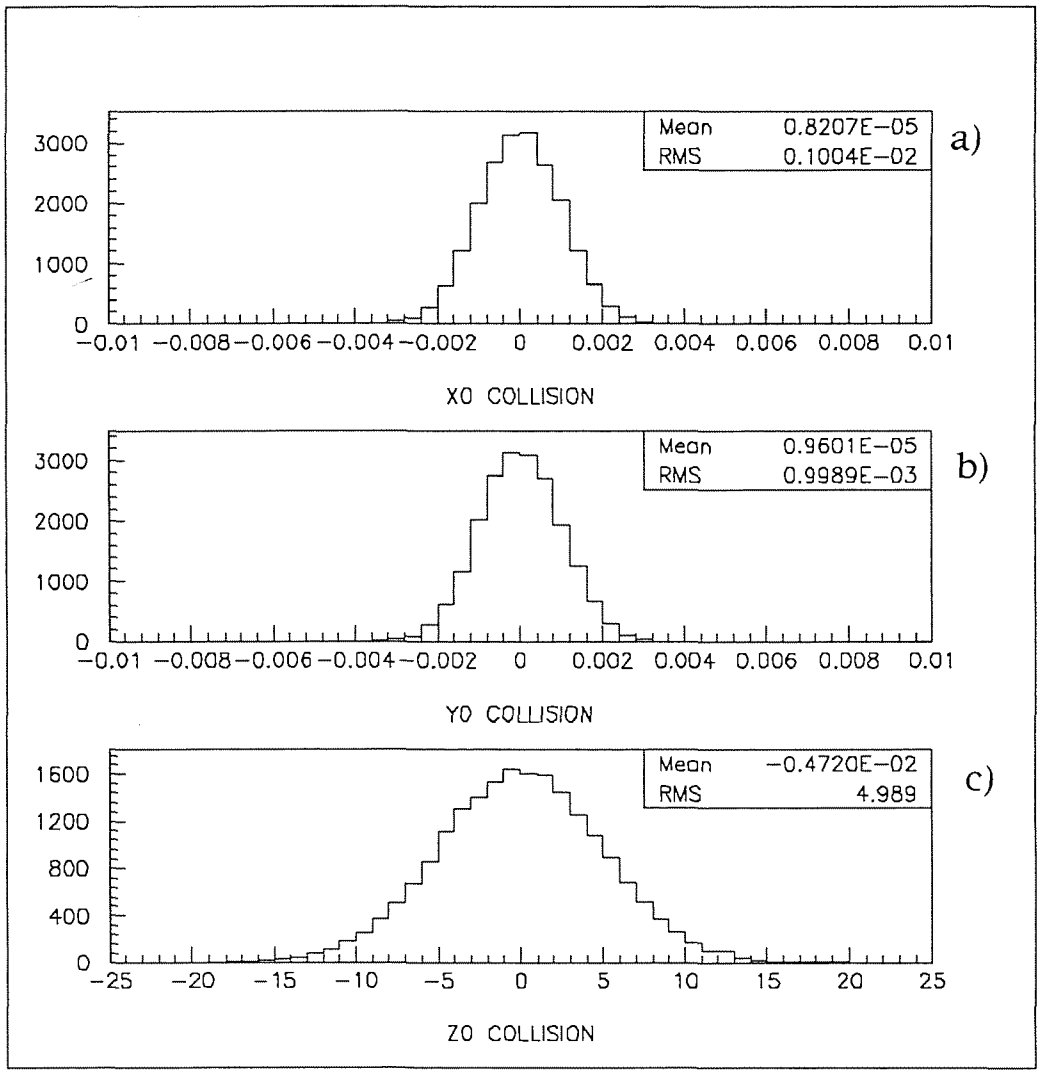
Mean 0.8207E-05
RMS 0.1004E-02
a)
3000
2000
1000
0
-0.01 -0.008 -0.006 -0.004 -0.002 0 0.002 0.004 0.006 0.008 0.01
X0 COLLISION
Mean 0.9601E-05
RMS 0.9989E-03
b)
3000
2000
1000
0
-0.01 -0.008 -0.006 -0.004 -0.002 0 0.002 0.004 0.006 0.008 0.01
Y0 COLLISION
Mean -0.4720E-02
RMS 4.989
c)
1600
1200
800
400
0
-25 -20 -15 -10 -5 0 5 10 15 20 25
Z0 COLLISION

Fig. 6

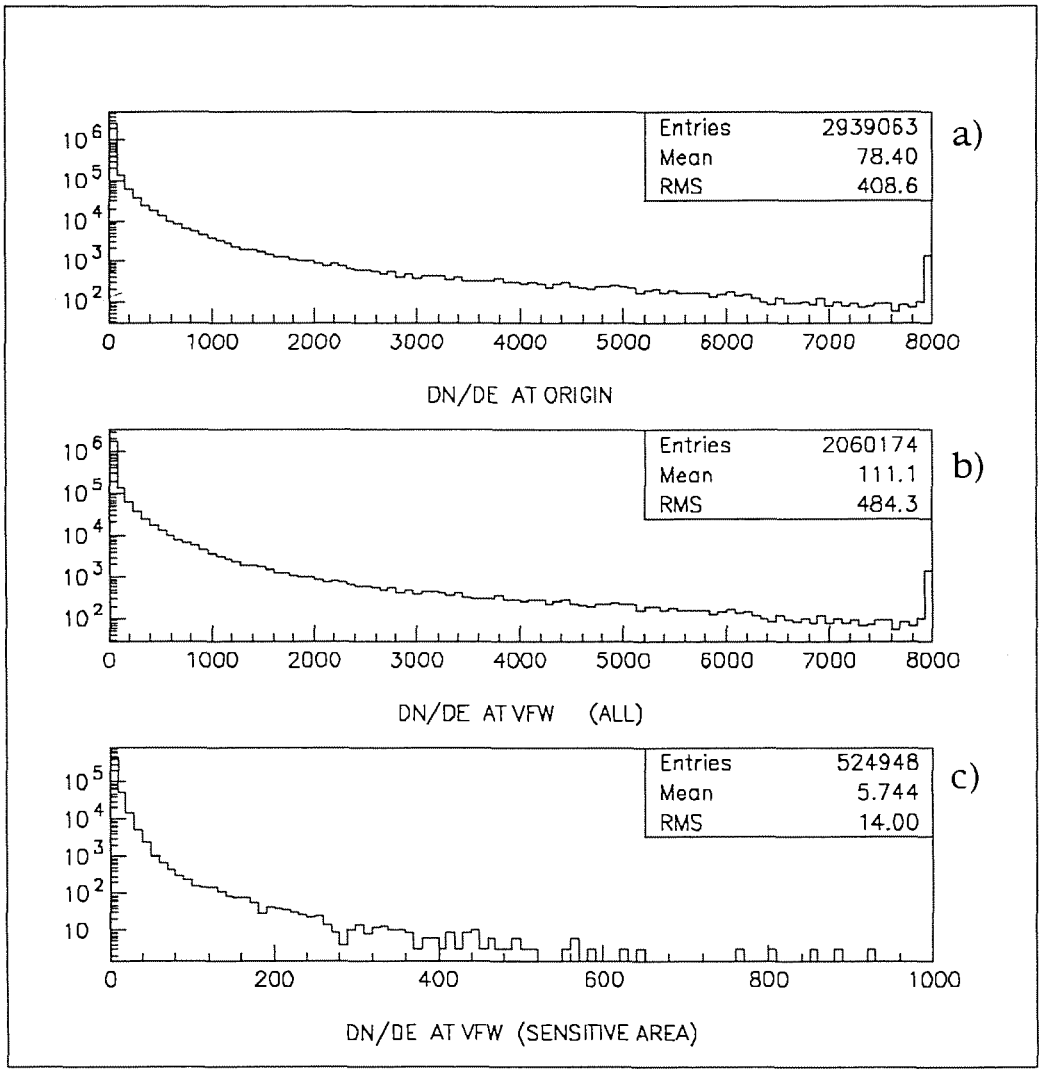
Entries 2939063
Mean 78.40
RMS 408.6
a)
DN/DE AT ORIGIN
Entries 2060174
Mean 111.1
RMS 484.3
b)
DN/DE AT VFW (ALL)
Entries 524948
Mean 5.744
RMS 14.00
c)
DN/DE AT VFW (SENSITIVE AREA)

Fig. 7

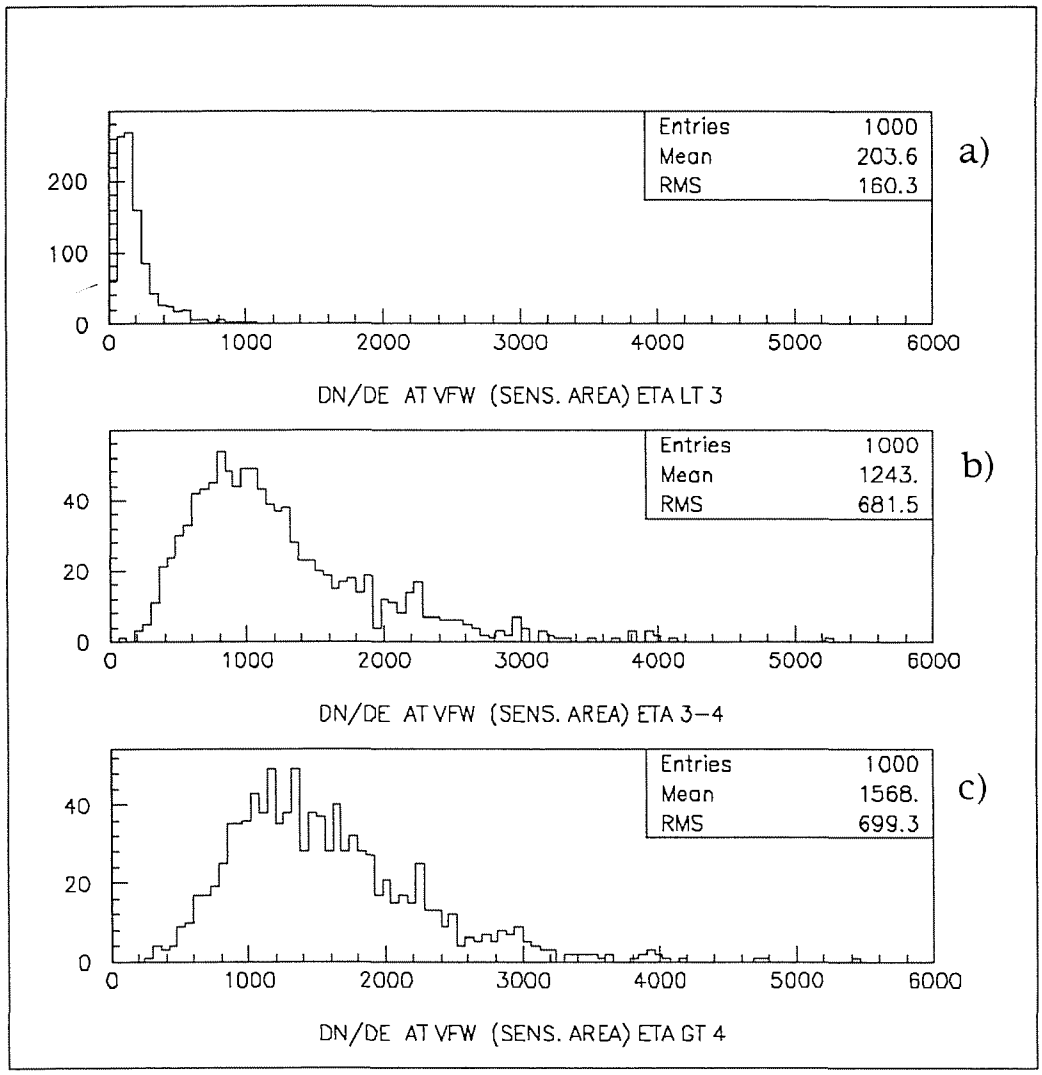
Entries 1000
Mean 203.6
RMS 160.3
a)
200
100
0
0 1000 2000 3000 4000 5000 6000
DN/DE AT VFW (SENS. AREA) ETA LT 3
Entries 1000
Mean 1243.
RMS 681.5
b)
40
20
0
0 1000 2000 3000 4000 5000 6000
DN/DE AT VFW (SENS. AREA) ETA 3-4
Entries 1000
Mean 1568.
RMS 699.3
c)
40
20
0
0 1000 2000 3000 4000 5000 6000
DN/DE AT VFW (SENS. AREA) ETA GT 4

Fig. 8

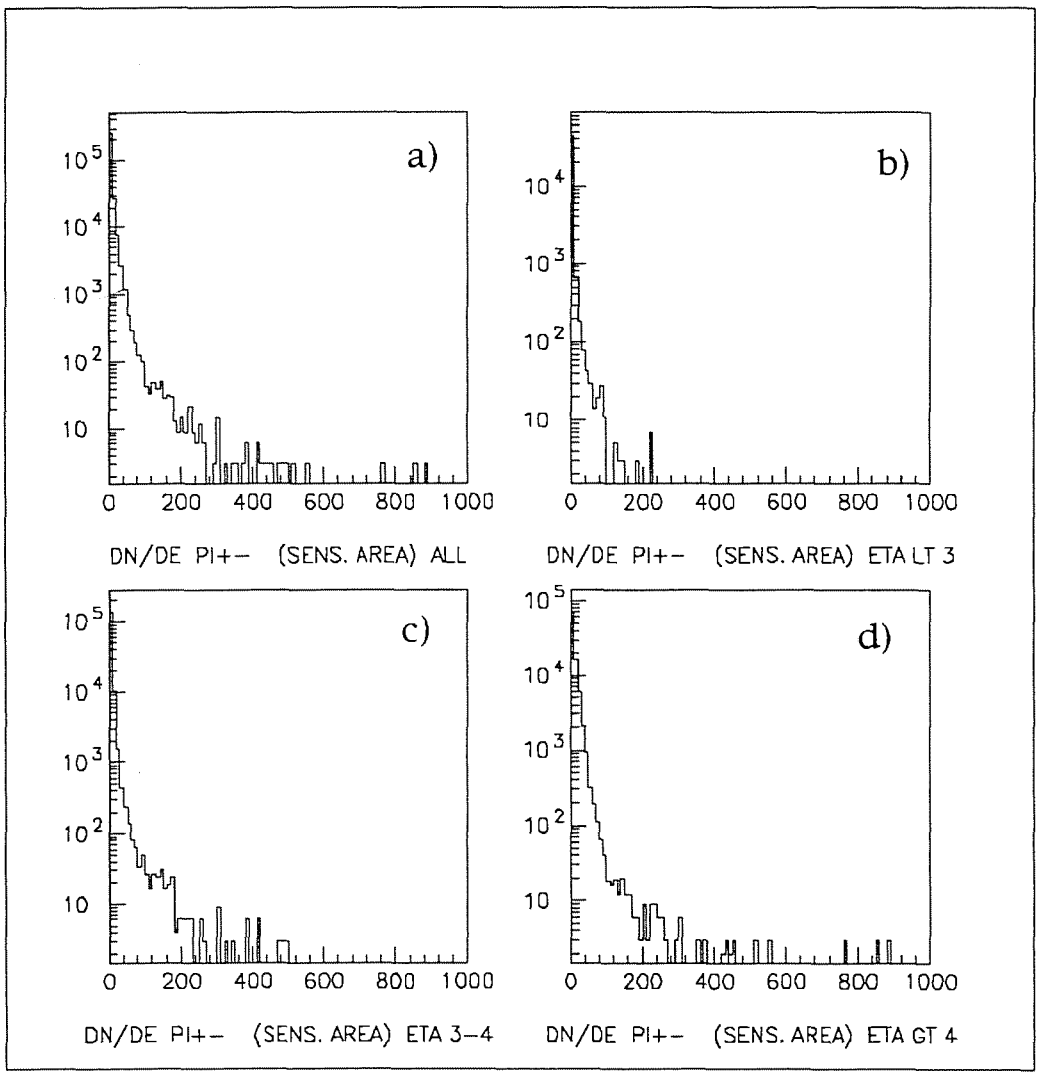
a)
b)
c)
d)
DN/DE PI+− (SENS. AREA) ALL
DN/DE PI+− (SENS. AREA) ETA LT 3
DN/DE PI+− (SENS. AREA) ETA 3−4
DN/DE PI+− (SENS. AREA) ETA GT 4

Fig. 9

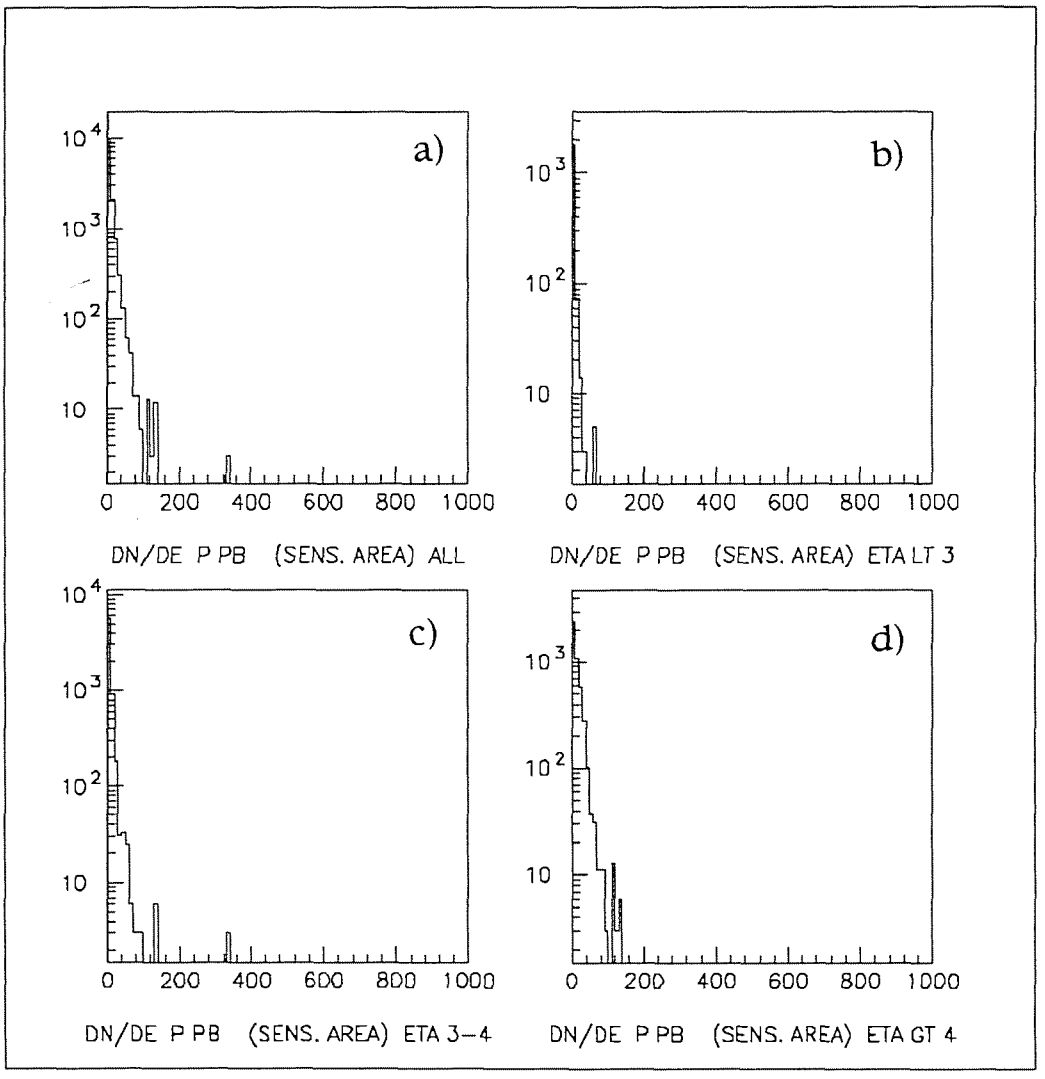
a)
b)
c)
d)
DN/DE P PB (SENS. AREA) ALL
DN/DE P PB (SENS. AREA) ETA LT 3
DN/DE P PB (SENS. AREA) ETA 3-4
DN/DE P PB (SENS. AREA) ETA GT 4

Fig. 10

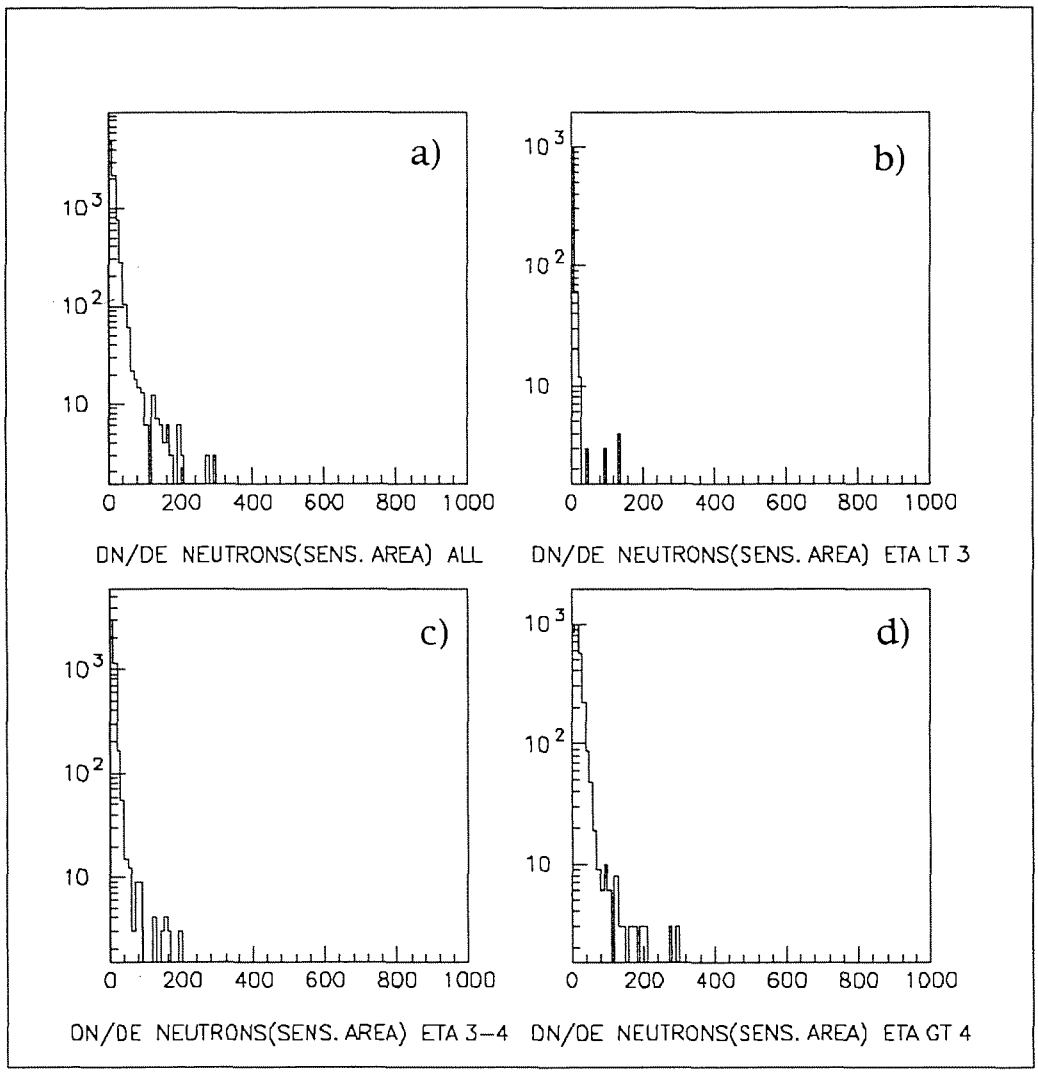
a)
b)
c)
d)
10^3
10^2
10
0
200
400
600
800
1000
DN/DE NEUTRONS(SENS. AREA) ALL
DN/DE NEUTRONS(SENS. AREA) ETA LT 3
DN/DE NEUTRONS(SENS. AREA) ETA 3-4
DN/DE NEUTRONS(SENS. AREA) ETA GT 4

Fig. 11

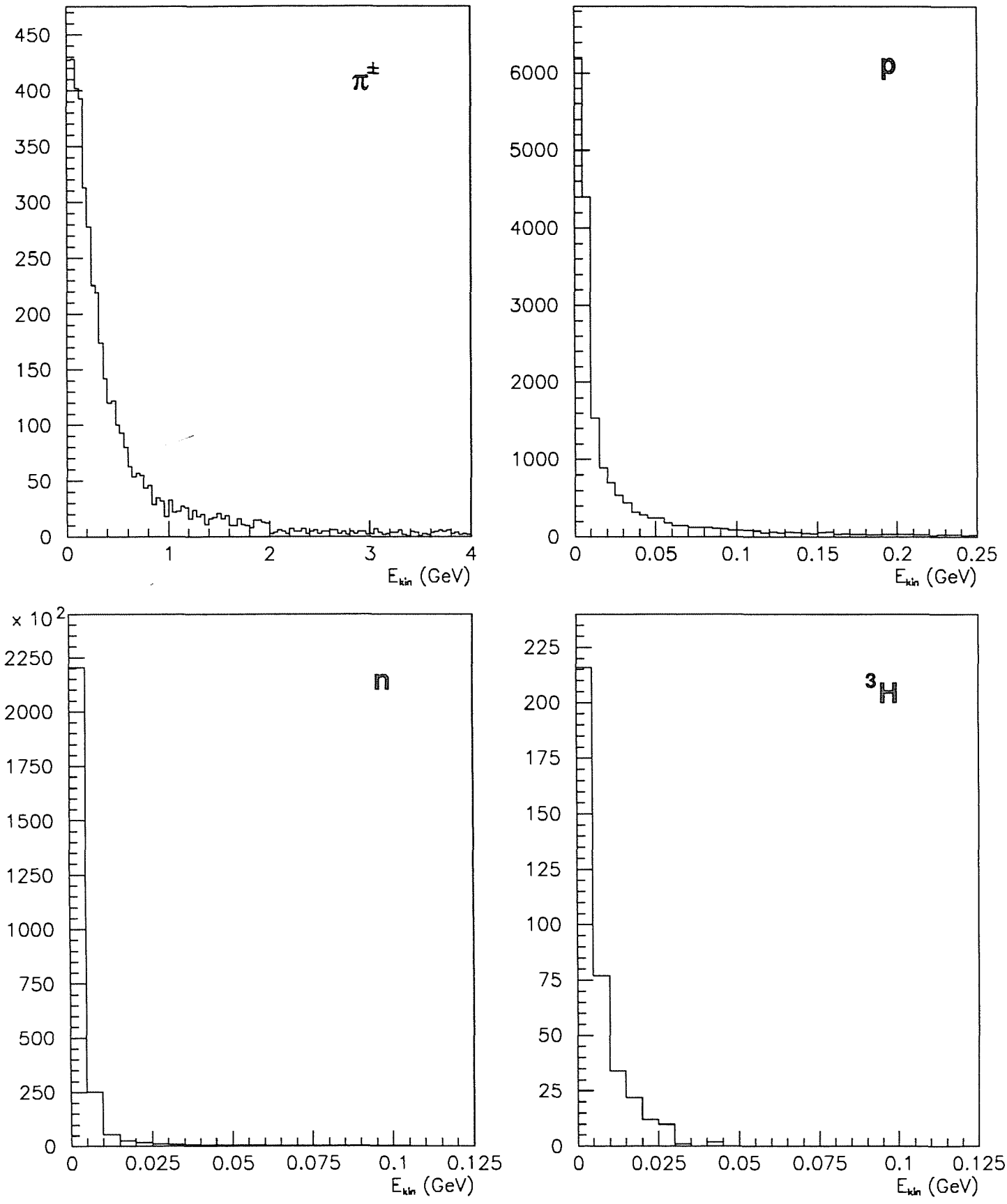

Fig. 12

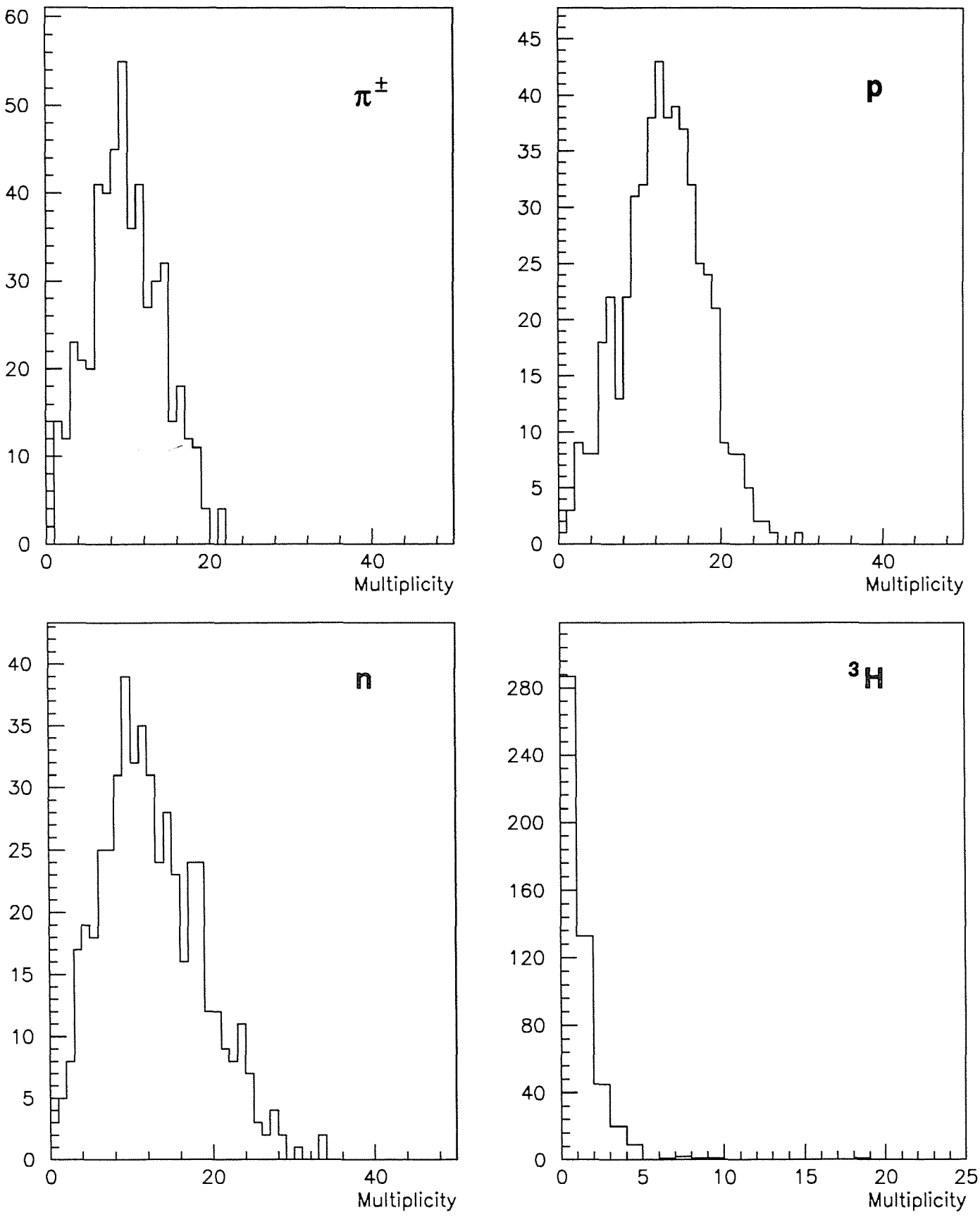
π±
Multiplicity
p
Multiplicity
n
Multiplicity
3H
Multiplicity

Fig. 13

CIEMAT-727

Centro de Investigaciones Energéticas, Medioambientales y Tecnológicas.
Instituto de Investigación Básica.- MADRID

Irradiación de un calorímetro muy delantero en las condiciones LHC: Algunas consecuencias."

FERRANDO, A.; JOSA, M.I.; MALININ, A.; MARTINEZ-LASO, L.; POJIDAEV, V.; SALICIO, J.M. (1994). 36 pp. 13 figs. 11 refs.

Hemos calculado el nivel de irradiación en la región muy delantera $(2.5 < |\eta| < 4.7)$ de un experimento LHC, usando el dispositivo CMS (Detector Solenoidal Compacto para LHC) propuesto. Hemos extraído información relativa a la radioactividad inducida en el absorbente del Calorímetro Muy Delantero de hierro/gas.

CLASIFICACION DOE Y DESCRIPTORES: 440200. 664300. Radiation Detectors. Calorimetry. Calorimeters. High Energy Physics. Irradiation. Hadons.

CIEMAT-727

Centro de Investigaciones Energéticas, Medioambientales y Tecnológicas.
Instituto de Investigación Básica.- MADRID.

"Irradiación de un calorímetro muy delantero en las condiciones LHC: Algunas consecuencias."

FERRANDO, A.; JOSA, M.I.; MALININ, A.; MARTINEZ-LASO, L.; POJIDAEV, V.; SALICIO, J.M. (1994). 36 pp. 13 figs. 11 refs.

Hemos calculado el nivel de irradiación en la región muy delantera $(2.5 < |\eta| < 4.7)$ de un experimento LHC, usando el dispositivo CMS (Detector Solenoidal Compacto para LHC) propuesto. Hemos extraído información relativa a la radioactividad inducida en el absorbente del Calorímetro Muy Delantero de hierro/gas.

CLASIFICACION DOE Y DESCRIPTORES: 440200. 664300. Radiation Detectors. Calorimetry. Calorimeters. High Energy Physics. Irradiation. Hadons.

CIEMAT-727

Centro de Investigaciones Energéticas, Medioambientales y Tecnológicas.
Instituto de Investigación Básica.- MADRID.

Irradiación de un calorímetro muy delantero en las condiciones LHC: Algunas consecuencias."

FERRANDO, A.; JOSA, M.I.; MALININ, A.; MARTINEZ-LASO, L.; POJIDAEV, V.; SALICIO, J.M. (1994). 36 pp. 13 figs. 11 refs.

Hemos calculado el nivel de irradiación en la región muy delantera $(2.5 < |\eta| < 4.7)$ de un experimento LHC, usando el dispositivo CMS (Detector Solenoidal Compacto para LHC) propuesto. Hemos extraído información relativa a la radioactividad inducida en el absorbente del Calorímetro Muy Delantero de hierro/gas.

CLASIFICACION DOE Y DESCRIPTORES: 440200. 664300. Radiation Detectors. Calorimetry. Calorimeters. High Energy Physics. Irradiation. Hadons.

CIEMAT-727

Centro de Investigaciones Energéticas, Medioambientales y Tecnológicas.
Instituto de Investigación Básica.- MADRID.

"Irradiación de un calorímetro muy delantero en las condiciones LHC: Algunas consecuencias."

FERRANDO, A.; JOSA, M.I.; MALININ, A.; MARTINEZ-LASO, L.; POJIDAEV, V.; SALICIO, J.M. (1994). 36 pp. 13 figs. 11 refs.

Hemos calculado el nivel de irradiación en la región muy delantera $(2.5 < |\eta| < 4.7)$ de un experimento LHC, usando el dispositivo CMS (Detector Solenoidal Compacto para LHC) propuesto. Hemos extraído información relativa a la radioactividad inducida en el absorbente del Calorímetro Muy Delantero de hierro/gas.

CLASIFICACION DOE Y DESCRIPTORES: 440200. 664300. Radiation Detectors. Calorimetry. Calorimeters. High Energy Physics. Irradiation. Hadons.

CIEMAT-727

Centro de Investigaciones Energéticas, Medioambientales y Tecnológicas.
Instituto de Investigación Básica.- MADRID

"Irradiation of a very forward calorimeter in the LHC environment: Some consequences."

FERRANDO, A.; JOSA, M.I.; MALININ, A.; MARTINEZ-LASO, L.; POJIDAEV, V.; SALICIO, J.M.
(1994). 36 pp. 13 figs. 11 refs.
We have computed the level of irradiation in the very forward region ($2.5 < |\eta| < 4.7$) 4.7) of an LHC experiment, using the proposed CMS (Compact Solenoidal Detector for LHC) setup. Information about the induced radioactivity in the absorber of a proposed iron/gas Very Forward Calorimeter has been extracted.

DOE CLASSIFICATION AND DESCRIPTORS: 440. 664300. Radiation Detectors. Calorimetry. Calorimeters. High Energy Physics. Irradiation. Hadons.

CIEMAT-727

Centro de Investigaciones Energéticas, Medioambientales y Tecnológicas.
Instituto de Investigación Básica.- MADRID.

"Irradiation of a very forward calorimeter in the LHC environment: Some consequences."

FERRANDO, A.; JOSA, M.I.; MALININ, A.; MARTINEZ-LASO, L.; POJIDAEV, V.; SALICIO, J.M.
(1994). 36 pp. 13 figs. 11 refs.
We have computed the level of irradiation in the very forward region ($2.5 < |\eta| < 4.7$) 4.7) of an LHC experiment, using the proposed CMS (Compact Solenoidal Detector for LHC) setup. Information about the induced radioactivity in the absorber of a proposed iron/gas Very Forward Calorimeter has been extracted.

DOE CLASSIFICATION AND DESCRIPTORS: 440. 664300. Radiation Detectors. Calorimetry. Calorimeters. High Energy Physics. Irradiation. Hadons.

CIEMAT-727

Centro de Investigaciones Energéticas, Medioambientales y Tecnológicas.
Instituto de Investigación Básica.- MADRID

"Irradiation of a very forward calorimeter in the LHC environment: Some consequences."

FERRANDO, A.; JOSA, M.I.; MALININ, A.; MARTINEZ-LASO, L.; POJIDAEV, V.; SALICIO, J.M.
(1994). 36 pp. 13 figs. 11 refs.
We have computed the level of irradiation in the very forward region ($2.5 < |\eta| < 4.7$) 4.7) of an LHC experiment, using the proposed CMS (Compact Solenoidal Detector for LHC) setup. Information about the induced radioactivity in the absorber of a proposed iron/gas Very Forward Calorimeter has been extracted.

DOE CLASSIFICATION AND DESCRIPTORS: 440. 664300. Radiation Detectors. Calorimetry. Calorimeters. High Energy Physics. Irradiation. Hadons.

CIEMAT-727

Centro de Investigaciones Energéticas, Medioambientales y Tecnológicas.
Instituto de Investigación Básica.- MADRID

"Irradiation of very forward calorimeter in the LHC environment: Some consequences."

FERRANDO, A.; JOSA, M.I.; MALININ, A.; MARTINEZ-LASO, L.; POJIDAEV, V.; SALICIO, J.M.
(1994). 36 pp. 13 figs. 11 refs.
We have computed the level of irradiation in the very forward region ($2.5 < |\eta| < 4.7$) 4.7) of an LHC experiment, using the proposed CMS (Compact Solenoidal Detector for LHC) setup. Information about the induced radioactivity in the absorber of a proposed iron/gas Very Forward Calorimeter has been extracted.

DOE CLASSIFICATION AND DESCRIPTORS: 440. 664300. Radiation Detectors. Calorimetry. Calorimeters. High Energy Physics. Irradiation. Hadons.